



Cite this: *RSC Adv.*, 2020, **10**, 45199

Design, synthesis and bioevaluation of novel 6-substituted aminoindazole derivatives as anticancer agents†

Ngo Xuan Hoang,^a Van-Hai Hoang,^b Thi-Thu-Trang Luu,^c Hung N. Luu,^d Thien Ngo,^f Duong Van Hieu,^a Nguyen Huu Long,^a Le Viet Anh,^a Son Tung Ngo,^d Yen Thi Kim Nguyen,ⁱ Byung Woo Han,ⁱ Thanh Xuan Nguyen,^j Dinh Thi Thanh Hai,^a Tran Thi Thu Hien^k and Phuong-Thao Tran^d                                            <img alt="ORCID iD icon" data-bbox="8

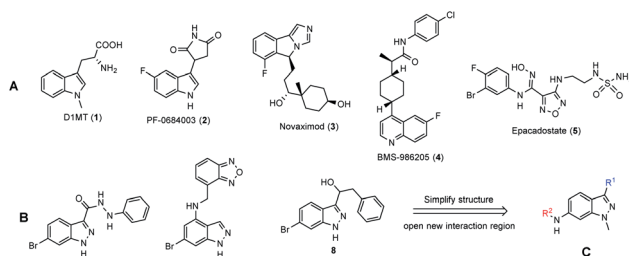


Fig. 1 (A) Clinical IDO1 inhibitors; (B) some IDO1 inhibitors bearing the indazole structure; (C) novel designed indazole derivatives.

currently in clinical trials.¹⁹ They have been generally combined with cytotoxic chemicals and immune checkpoint agents on clinical trials.^{19,20} The combined therapies improved the efficacy on the tumors of immune checkpoint and cytotoxic agents in both preclinical^{21,22} and clinical studies.²³ The benefits come from the ability to restore immunosurveillance and blunt tumor neovascularization *via* re-programming inflammatory processes.²⁴ However, the combination of two drugs is able to cause drawbacks, such as drug–drug interactions, different pharmacokinetics and inconveniences in pharmaceutics and treatment.²⁵ Therefore, a new “multitarget” concept was enunciated for complex diseases such as cancer.^{25,26} Based on this new concept, a few X/IDO1 dual inhibitors were reported, such as HDAC/IDO1 dual inhibitors²⁷ and DNA/IDO1 dual targeting agents.²⁸

Indazole is an important scaffold in drug discovery, which is present in different anticancer agents. Most of them are receptor tyrosine kinase- (EGFR, FGFR, VEGFR) or serine/threonine kinase (aurora kinase, cyclin-dependent kinase) inhibitors.^{29–31} The diversity comes from the structure, in which two nitrogen atoms can tautomerize and can be introduced to different groups. In addition, indazole, a bioisostere of the indole ring in tryptophan, was used as the skeletal structure for design new IDO1 inhibitors.^{32–35} Indazoles bearing 3-hydrazide groups (6)³² were first studied in 2016 with IC_{50} values near the nanomolar range. Next, some 4-amino (7)^{33,34} and 3-(hydroxymethyl) (8) indazoles were also reported as IDO1 inhibitors at the sub-nanomolar range (Fig. 1B). To date, all indazole derivatives bear a huge group at position 4 and a small group (normally a halogen) at position 6.

In this study, we chose indazole as the core structure for the rational design of new IDO1- and cytotoxic agents. We simplified and considered the derivatization abilities of the indazole structure, and then synthesized a library of 6-substituted aminoindazoles (Fig. 1C). Next, we evaluated their toxicities on five cancer cell lines and investigated the IDO1 inhibitory activities *in vitro*. We further performed docking studies to calculate the binding energy and analyzed the specific binding interactions between the selected inhibitors and the IDO1 active site. Finally, we examined the potential mechanisms of the most active compound on the cell cycle arrest in human colorectal cancer cells.

Results and discussion

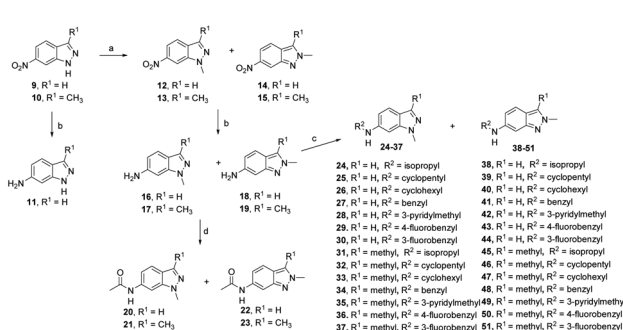
Chemistry

The synthesis of 6-substituted-indazole derivatives was performed, as illustrated in Scheme 1. Briefly, 6-nitro indazole derivatives **9**, **10** were methylated by iodomethane using potassium carbonate in DMF to get two isomers: the major products, *N*¹-alkylindazoles **12**, **13** and the minor products *N*²-alkylindazoles **14**, **15**. The structures of two isomers were confirmed by 2D-NMR before carrying out a reduction reaction under hydrogen gas to afford corresponding 6-amino indazole derivatives **11**, **16–19**. Next, the amines were reductively aminated with a ketone or an aldehyde in the presence of a mild and selective reductive agent, namely sodium cyanoborohydride, to afford secondary amines **24–51**. Moreover, acetamide derivatives **20–23** were prepared from the corresponding amine and acetic anhydride under basic conditions.

Anti-proliferative activity

The as-synthesized indazole derivatives were evaluated for the *in vitro* anti-proliferative activity in five different cancer cell lines including HCT116, A549, SK-HEP-1, SNU-638, and MDA-MB-231 using the sulforhodamine B method. Etoposide was used as the positive control. The results are summarized in Tables 1 and 2.

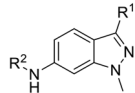
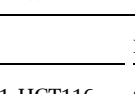
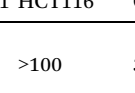
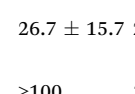
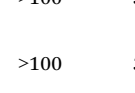
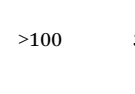
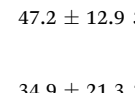
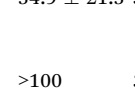
First, we examined the structure–activity relationship (SAR) of the as-synthesized compounds on colon cancer cell (HCT116) proliferation, in which required IDO activation increases the expression of β -catenin and its targeting genes including cyclin D and Axin2 for development.³⁶ As demonstrated in Tables 1 and 2, the introduction of a methyl group at the C-3 position of the indazole ring **33–37** caused a potential toxicity against HCT116. Among them, the substitution of an aryl group in indazoles **34–37** showed a better cytotoxicity than the cyclohexyl-substituted compound **33**. A replacement of benzyl by 3-pyridylmethyl **35** or fluorobenzyl **36**, **37** increased the toxic potency from 2.7 to 18.8-fold as compared to **34**. Of note, compound **36** had a great anti-proliferative activity ($IC_{50} = 0.4 \pm 0.3 \mu\text{M}$), which indicates the importance of the fluoro group.



Scheme 1 Reagents and conditions: (a) CH_3I (2.0 equiv.), excess K_2CO_3 , DMF, 60 °C, 4 h, 95–98%; (b) H_2 , Pd/C (10 mol%), r.t., 4 h, 85–96%; (c) ketone or aldehyde (1.0 equiv.), NaBH_3CN (5.0 equiv.), AcOH , MeOH , 40 °C, 4 h, 73–96%; (d) excess Ac_2O , TEA, DMC, r.t., 2 h, 89–92%.



Table 1 Cytotoxicity of N^1 -methyl indazole derivatives on five cell lines

R^2	$R^1 = H$ (IC_{50}^a (μM))						$R^1 = CH_3$ (IC_{50}^a (μM))					
	Cpd	A549	SK-HEP-1	SNU-638	MDA-MB-231	HCT116	Cpd	A549	SK-HEP-1	SNU-638	MDA-MB-231	HCT116
	24	>100	>100	>100	>100	>100	31	>100	>100	>100	>100	>100
	20	>100	>100	>100	>100	26.7 \pm 15.7	21	>100	>100	>100	>100	>100
	25	>100	>100	64.8 \pm 28.4	>100	>100	32	>100	36.8 \pm 11.2	3.8 \pm 3.9	>100	>100
	26	>100	>100	>100	>100	>100	33	27.0 \pm 18.7	39.6 \pm 22.4	13.7 \pm 9.1	>100	14.5 \pm 16.3
	27	>100	>100	>100	>100	>100	34	5.1 \pm 23.3	28.1 \pm 20.0	1.9 \pm 2.0	>100	7.5 \pm 5.0
	28	19.8 \pm 6.1	>100	>100	>100	47.2 \pm 12.9	35	30.0 \pm 18.5	33.9 \pm 22.6	>100	>100	2.7 \pm 2.3
	29	0.7 \pm 0.1	>100	1.2 \pm 1.2	>100	34.9 \pm 21.3	36	6.8 \pm 2.4	50.1 \pm 23.4	1.8 \pm 2.2	47.5 \pm 8.4	0.4 \pm 0.3
	30	19.9 \pm 10.6	>100	1.3 \pm 1.0	>100	>100	37	>100	42.2 \pm 15.0	2.5 \pm 2.6	81.7 \pm 25.2	2.2 \pm 0.9
Etoposide		0.27 \pm 0.1	0.30 \pm 0.1	0.61 \pm 0.2	7.35 \pm 2.3	1.27 \pm 0.8						

^a IC_{50} : the concentration (μM) of compounds that produces a 50% reduction cell growth. All the data were calculated from the experiments conducted in triplicate and repeated at least three times. Data represent mean \pm SD.

Changing the position of the fluoro group from *para* to *meta* caused a 5.5 times activity drop. In contrast, introducing alkyl groups to **31**, **32** resulted in non-toxic compounds. Similarly, the toxicity of acetamide derivative **21** was abolished. Removing the methyl group from the C-3 position of the indazole ring caused a reduction in the toxicity against HCT116, except for the acetylated compound **20** ($IC_{50} = 26.7 \pm 15.7 \mu M$). Besides, relocating the methyl group from N^1 to N^2 decreased the anti-proliferative activity of most of the compounds (Table 2), excluding isopropyl- and acetyl compounds. In particular, compound **22** showed a potent activity with an IC_{50} value of $2.5 \pm 1.6 \mu M$. The most effective groups, 3-pyridylmethyl **49**, 4-fluorobenzyl **50** and 3-fluorobenzyl **51**, demonstrated less cytotoxicity of 5.8 to 34.5-fold than the corresponding N^1 -methyl isomers. Overall, the absence of the methyl group at the 3-position in the indazole ring favored a small alkyl- or an acetyl-substituted group in displaying the anti-proliferative activity. In contrast, the substitution of an aryl group preferred 3-methylindazole compounds in presenting cytotoxic activities.

Next, the SAR of all as-synthesized compounds against the other four cell lines including A549, SK-HEP-1, SNU-638, and MDA-MB-231 (Tables 1 and 2) was examined. Most of them showed a mild suppressive effect on SK-HEP-1 and MDA-MB-231 ($IC_{50} > 20 \mu M$) excluding compounds **39**, **49**, **50**. We observed that compound **39** had a great suppressive potency on

MDA-MB-231, A549, and SNU-638 cells with $IC_{50} = 1.7 \pm 1.1$, 2.8 ± 1.3 , and $1.8 \pm 1.4 \mu M$, respectively.

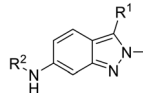
In addition, the *N*-aromatic substitution of 6-aminoindazole derivatives **29**, **30**, **34**, **36**, **37** exhibited considerable cytotoxicity towards A549 and SNU-638 cancer cell lines with IC_{50} values ranging from 0.7 to $10 \mu M$. The cytotoxicity changed dramatically among substituted groups. Moreover, there was no correlation between the cytotoxicity and structure observed. In addition, the IC_{50} values of compounds **22**, **34**–**37** on the normal cell MRC5 were higher than the IC_{50} of them on HCT116 cancer cell line. Specially, compound **36** demonstrated 29.6-fold selectivity against HCT116 than MRC5 (Table S1 – ESI file†).

IDO1 inhibition assay

In order to examine the effects on IDO1 expression, which can be well correlated to human colon cancer cell growth,^{37,38} we selected the compounds with the most anti-proliferative potency against HCT116 for the analysis of the IDO1-suppressive activity (Fig. 2). We found that at the concentration of $10 \mu M$, the expression of IDO1 in HCT16 cells seemed unaffected by compound **35** or **37** (Fig. 2); moreover, it was suppressed by a treatment with compound **22** or **36** (Fig. 2). Furthermore, the effects of compound **36** on IDO1 expression were observed in a concentration-dependent manner (Fig. 3 and S2 – ESI file†).



Table 2 Cytotoxicity of N^2 -methyl indazole derivatives on five cell lines

											
R^2	$R^1 = H$ (IC_{50}^a (μM))					$R^1 = CH_3$ (IC_{50}^a (μM))					
	Cpd A549	SK-HEP-1	SNU-638	MDA-MB-231	HCT116	Cpd A549	SK-HEP-1	SNU-638	MDA-MB-231	HCT116	
	38	38.9 ± 13.2	>100	30.4 ± 27.0	68.3 ± 27.3	33.4 ± 11.7	45	>100	>100	>100	>100
	22	58.7 ± 23.9	>100	>100	20.6 ± 1.7	2.5 ± 1.6	23	>100	>100	>100	>100
	39	1.8 ± 1.4	>100	2.8 ± 1.3	1.7 ± 1.1	>100	46	>100	>100	>100	>100
	40	37.4 ± 10.2	>100	>100	>100	>100	47	37.0 ± 22.7	32.7 ± 11.2	33.0 ± 17.5	26.1 ± 13.8
	41	>100	>100	>100	>100	49.7 ± 3.6	48	>100	>100	>100	>100
	42	>100	>100	>100	>100	>100	49	>100	>100	19.4 ± 17.0	19.1 ± 13.5
	43	>100	>100	63.3 ± 13.8	>100	>100	50	19.4 ± 20.6	37.3 ± 6.3	10.8 ± 11.2	8.0 ± 1.7
	44	>100	>100	>100	>100	>100	51	>100	>100	61.3 ± 32.3	12.7 ± 8.5
Etoposide		0.27 ± 0.1	0.30 ± 0.1	0.61 ± 0.2	7.35 ± 2.3	1.27 ± 0.8					

^a IC_{50} : the concentration (μM) of compounds that produces a 50% reduction cell growth. All the data were calculated from the experiments conducted in triplicate and repeated at least three times. Data represent mean \pm SD.

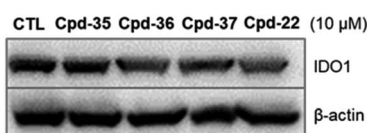


Fig. 2 Effect of 6-substituted aminoindazole derivatives on the IDO1 expression in human colorectal cancer cells. HCT116 were treated with 10 μM of indicative compounds for 24 h. The immunoblotting analysis was performed to determine IDO1 and β -actin expression.

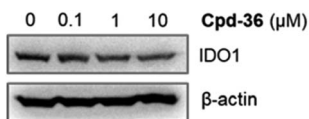


Fig. 3 HCT116 cells were treated with compound 36 at various concentrations. The immunoblotting analysis was performed to determine IDO1 and β -actin protein levels.

Docking simulation analysis of IDO1 and its inhibitors

To gain insight into the interaction between inhibitors and IDO1, we performed molecular docking simulation studies on

the active site region of IDO1. To validate the docking program Autodock Vina, we performed a control docking experiment with the 5PK compound in the IDO1 complex structure (PDB ID: 5EK3). 5PK was predicted to dock into the active site of IDO1 as in the actual complex structure with a binding energy of -9.5 kcal mol $^{-1}$ (described in Fig. S1 of the ESI file[†]). We found that both compounds 35 and 36 bound to IDO1 in a comparable way to that of the 5PK-IDO1 complex structure (Fig. 4A). In addition, the binding energy of compound 35 (-8.1 kcal mol $^{-1}$) was higher than that of compound 36 (-8.9 kcal mol $^{-1}$), suggesting a higher binding affinity towards IDO1 of compound 36 than that of compound 35. In the docking model, compounds 35 and 36 were recognized and/or stabilized by well-known active site residues Tyr126, Phe163, Phe164, Ser167, Phe226, Phe227, Arg231, Ser263, and His346,³⁹ which play a similar role in the 5PK-IDO1 complex structure (Fig. 4B). The docking models showed that the N^2 indazole group of compound 36 formed a hydrogen bond with the hydroxy group of Ser167, and the fluorophenyl/pyridinyl ring formed a π - π interaction with Phe226 (Fig. 4C). In addition, the 6-NH group in the compounds also formed a hydrogen bond with the 7-propionate of the heme ion (Fig. 4C).



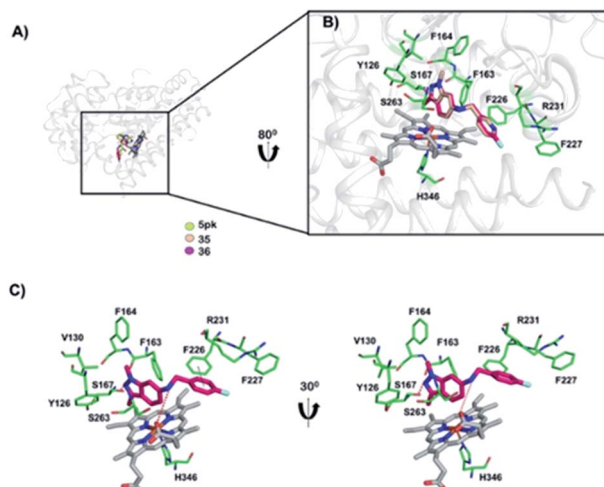


Fig. 4 Docking model of IDO1 with 5PK and compounds. (A) The docking models of 5PK, compound **35**, and compound **36** are shown in yellow green, light yellow, and pink models, respectively. (B) A close-up view of docked compounds in the active site cavity of IDO1. (C) The interaction mode of IDO1 with compound **36**. The IDO1 residue recognizing ligands are shown in the green stick model. The heme ion is shown in a grey stick. Hydrogen bonds and π - π interactions are shown in red and black dots, respectively.

Study mechanism of compound **36** on human colorectal cancer cells

Compound **36** demonstrated a concentration-dependent suppressive effect on the activity of the HCT116 viability (Fig. 5). On other cell lines, despite a modest effect on the IDO expression, compound **36** still demonstrated a remarkable inhibition of cell viability. This phenomenon suggested that other mechanisms may also be responsible for the anti-proliferative effect of compound **36**. Therefore, to further explore the possible mechanism of action of the anti-proliferative activity of compound **36**, the effect of compound **36** on the modulation of the cell cycle was determined.

A cell cycle analysis indicated that a treatment with 10 μ M of compound **36** stimulated the G2/M cell cycle arrest in HCT116 cells within 24 h of post-treatment (Fig. 6A). Furthermore, a concentration-dependent concentration simulative effect on the G2/M cell cycle arrest was observed at 48 h after the

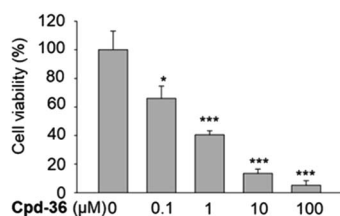


Fig. 5 Anti-proliferative effect of compound **36** on HCT116 cells. HCT116 cells were treated with compound **36** at various concentrations for 72 h, and cell proliferation was determined by the SRB assay. The data were presented as mean \pm SD. The experiment was performed in triplicate ($n = 3$).

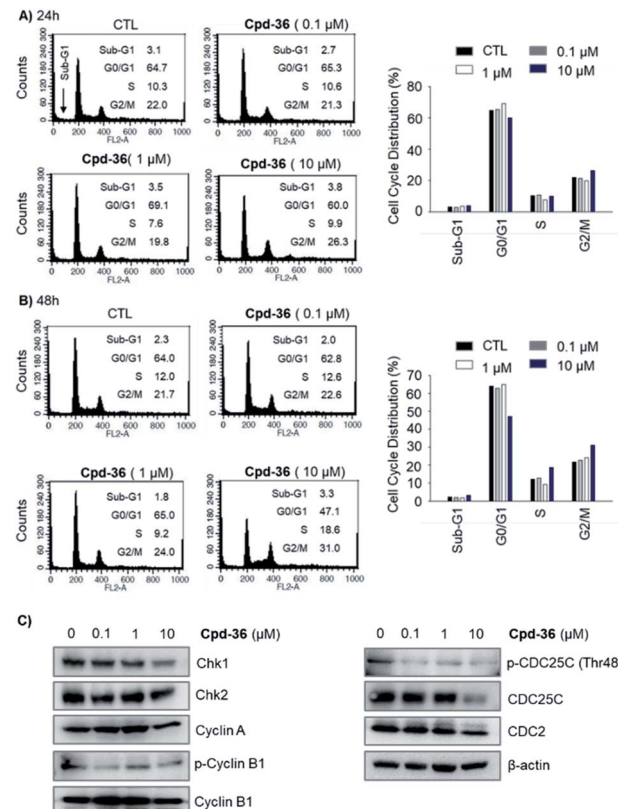


Fig. 6 Effect of compound **36** on the cell cycle distribution in human colorectal cancer cells. (A and B) HCT116 cells were treated with compound **36** for 24 h or 48 h. The cell cycle distribution was analyzed via flow cytometry. (C) Effects of **36** on the expression of cell cycle-related proteins in HCT116 cells. HCT116 cells were treated with **36** for 48 h. Subsequently, the protein expression levels of cell cycle-related proteins were analyzed by the immunoblotting assay.

treatment (Fig. 6B). We further analyzed the expression of the G2/M cell cycle regulatory proteins by immunoblot. We found that the expression of p-CDC25C (Thr⁴⁸), CDC25C, Chk1, and p-cyclin B1 were down-regulated (Fig. 6C). These findings suggested that the anti-proliferative activity of compound **36** was associated, at least partially, with the G2/M phase cell cycle arrest through regulating cell cycle modulators in human colorectal cancer cells.

Experimental section

Chemistry

All chemical reagents were commercially available and used directly without any purification. Thin layer chromatography, which was performed using Whatman® 250 μ m Silica Gel GF Uniplates and visualized under UV light at 254 nm, was used to check the progress of reactions and preliminary evaluation of the homogeneity of the compounds. In all cases, the compounds achieved a purity of 97% or above as determined by HPLC. Melting points were measured using a Gallenkamp Melting Point Apparatus (LabMerchant, London, United Kingdom) and were uncorrected. The purification of



compounds was carried out using crystallization methods and/or open silica gel column flash chromatography employing Merck silica gel 60 (240 to 400 mesh) as the stationary phase. Nuclear magnetic resonance spectra (^1H NMR, ^{13}C NMR) were recorded on a JEOL JNM-LA 300 at 300 MHz and Bruker Analytik, DE/AVANCE Digital 500 at 500 and 125 MHz spectrometers. Tetramethylsilane was used as the internal standard. Chemical shifts were reported in parts per million (ppm) downfielded from tetramethylsilane. Mass spectra with different ionization modes including electron ionization (EI) and electrospray ionization (ESI) were recorded using PE Biosystems API2000 (PerkinElmer, Palo Alto, CA, USA) and Mariner® (Azco Biotech, Inc. Oceanside, CA, USA) or LC-MSD-Trap-SL (Agilent, CA, USA) mass spectrometers. All reagents and solvents were purchased from Aldrich or Fluka Chemical Corp. (Milwaukee, WI, USA) or Merck unless noted otherwise. Solvents were used directly as purchased unless otherwise indicated.

General procedure for methylation (procedure 1). To a mixture of 6-nitroindazole derivative (1.0 equiv.) and excess potassium carbonate in dry DMF was added iodomethane (2.0 equiv.) and stirred at 60 °C for 4 h. The reaction mixture was quenched with water and extracted with EA (3 times). The organic layer was collected, washed with water and brine, concentrated, and purified by silica gel column chromatography using ethyl acetate/*n*-hexane (1/2) as the mobile phase to get the two isomers: *N*¹-methylation (major, less polar) product and *N*²-methylation (minor, more polar) product.

General procedure for reduction (procedure 2). The nitroindazole compound was dissolved in MeOH or THF and then 10% Pd/C was added. The mixture was stirred at room temperature under hydrogen gas atmosphere for 4 h. The crude mixture was filtered through Celite, and washed by MeOH. The solution was concentrated and used for the next step without any purification.

General procedure for reductive amination (procedure 3). A mixture of amine (1.0 equiv.), aldehyde or ketone (1.0 equiv.) and acetic acid (5.0 equiv.) in MeOH was stirred for 5 min, and then NaBH₃CN (5.0 equiv.) was added. The reaction mixture was stirred at 40 °C for 4 h, and then diluted with DCM. The organic layer was washed using a bicarbonate solution and water, then concentrated, and purified *via* silica gel column chromatography using ethyl acetate/*n*-hexane (1/5 to 1/1) as the mobile phase.

General procedure for acetylation (procedure 4). Excess amount of acetic anhydride was added into a solution of amine and TEA in DCM. The reaction mixture was stirred at room temperature for 2 h and diluted with DCM. The organic solution was washed with the bicarbonate solution and water, and then purified *via* silica gel column chromatography using ethyl acetate/*n*-hexane (1/3) as the mobile phase.

Cell culture

Human colorectal cancer cells (HCT116), gastric cancer cells (SNU638), breast cancer cells (MDA-MB-231), liver cancer cells (SK-HEP-1) were purchased from American Type Culture

Collection (Manassas, VA, USA). HCT116, SNU638, MDA-MB-231, SK-HEP-1 were cultured, as described previously.⁴⁰

Sulforhodamine B assay

The effect of the indicated compounds on cell proliferation was calculated as described previously.⁴⁰ In brief, HCT116 cells (2×10^4 cells per mL) were seeded in 96-well plates with different compounds. After incubation, the cells were fixed with a 50% trichloroacetic acid (TCA) solution for 1 h, and cellular proteins were stained with 0.4% sulforhodamine B (SRB) in 1% acetic acid. The stained cells were dissolved in 10 mM Tris buffer (pH 10.0). The effect of the investigated compound on cell proliferation was calculated as a percentage relative to a solvent-treated control, and the IC₅₀ values were evaluated *via* nonlinear regression analysis (percent survival *versus* concentration). Etoposide was used as the positive control.

Flow cytometry for cell cycle analysis

HCT116 cells (2×10^5 cells per mL) were plated in a 36 mm culture dish and incubated for 24 h. A fresh medium containing the indicated concentration of compound 36 was added to culture dishes. Following a 24 h or 48 h incubation, the cells were harvested (*via* trypsinization and centrifugation), rinsed twice with pre-cooled phosphate buffered saline (PBS), and prepared for the cell cycle analysis as described previously.⁴⁰

Western blot analysis

HCT116 cells (2×10^5 cells per mL) were treated with various concentrations of 36 for the indicated times. Western blot analysis was carried out as described previously.⁴¹ The antibody for IDO1 (ab55305) was purchased from Abcam (Abcam, Cambridge, UK). Antibodies for CDC25C, phosphor-CDC25C (Thr⁴⁸), Chk1, Chk2, and phosphor-cyclin B1 (Ser¹⁴⁷) were purchased from Cell Signaling Technology (Danvers, MA, USA). Antibodies for cyclin A (H-432), CDC2, cyclin B1 (H-433), and β -actin (C4) were purchased from Santa Cruz Biotechnology (Santa Cruz, CA, USA).

Statistical analysis

All experiments were repeated at least three times. The data are shown as the means \pm standard deviation (SD) for the indicated number of independently performed experiments. The student's *t*-test was used for the determination of statistical significance, and IC₅₀ values were determined by nonlinear regression using the Sigma Plot (Systat Software, Inc., San Jose, CA, USA). The difference was considered statistically significant when *p* (*) < 0.05, (**) < 0.001, (***) < 0.0001.

Molecular simulation docking

The structure of IDO1 was acquired from the protein data bank (PDB ID: 5EK3), and the structure of compound 35 and compound 36 were drawn by the ChemDraw program (version Pro 16.0, Cambridge soft, Cambridge, MA). The structure of the control compound 5PK was extracted from the complex structure of 5PK-IDO1 (PDB ID: 5EK3). The compounds were docked



into the active site region of IDO1 using AutoDock Vina (version 1.1.2, La Jolla, CA, USA)⁴² with a grid map defined in $20 \times 20 \times 20 \text{ \AA}^3$ dimensions to contain the proposed active sites and hem, which are essential for the enzyme activity.⁴³ The conformations of the ligands and receptors were fixed. The program was run in score mode with an exhaustiveness value of 20.

Conclusions

In summary, four series of 6-substituted aminoindazoles were designed based on an anticancer privileged structure, indazole, targeting to inhibit the IDO1 activity, and the designed compounds were synthesized through 3 steps. Of them, the acetyl, pyridinylmethyl, and fluorobenzyl substituted compounds (22, 35–37) showed potential cytotoxicity towards colorectal cancer cells HCT116. A study on the IDO1 activity indicated that compound 36 had a moderate inhibition activity of IDO1 towards the HCT116 cell line. The molecular modeling analysis showed that compound 36 fitted well to the IDO1 active site and created hydrogen bonds with Ser167 and 7-propionate in the heme structure. Further studies indicated that compound 36 arrested the G2/M cell cycle of HTC116 through regulating the cell cycle modulators. Due to the good cytotoxicity on colorectal cancer cells, and having a small structure, we believe that compound 36 might be useful for the design of new anti-cancer agents.

Conflicts of interest

There are no conflicts to declare.

Acknowledgements

This research was funded by the Vietnam National Foundation for Science and Technology Development (NAFOSTED) under grant number 108.05-2020.01. We would like to thank Professor Sang Kook Lee and Dr Duc-Hiep Bach (College of Pharmacy, Natural Products Research Institute, Seoul National University, Seoul 08826, Republic of Korea) for the biological part.

References

- D. H. Bach, D. Kim, S. Y. Bae, W. K. Kim, J. Y. Hong, H. J. Lee, N. Rajasekaran, S. Kwon, Y. Fan, T. T. Luu, Y. K. Shin, J. Lee and S. K. Lee, *Mol. Ther.-Nucleic Acids*, 2018, **11**, 455–467.
- D. H. Bach, T. T. Luu, D. Kim, Y. J. An, S. Park, H. J. Park and S. K. Lee, *Mol. Ther.-Nucleic Acids*, 2018, **12**, 817–828.
- D. Kim, D. H. Bach, Y. H. Fan, T. T. Luu, J. Y. Hong, H. J. Park and S. K. Lee, *Cell Death Dis.*, 2019, **10**, 361.
- T. T. Luu, D. H. Bach, D. Kim, R. Hu, H. J. Park and S. K. Lee, *Anticancer Res.*, 2020, **40**, 1855–1866.
- P. T. Huong, L. T. Nguyen, X. B. Nguyen, S. K. Lee and D. H. Bach, *Cancers*, 2019, **11**, 240.
- D. H. Bach, J. Y. Hong, H. J. Park and S. K. Lee, *Int. J. Cancer*, 2017, **141**, 220–230.
- N. P. Restifo, M. J. Smyth and A. Snyder, *Nat. Rev. Cancer*, 2016, **16**, 121.
- J. Tang, L. Pearce, J. O'Donnell-Tormey and V. M. Hubbard-Lucey, *Nat. Rev. Drug Discovery*, 2018, **17**, 783–784.
- P. Sharma, S. Hu-Lieskován, J. A. Wargo and A. Ribas, *Cell*, 2017, **168**, 707–723.
- A. Botticelli, B. Cerbelli, L. Lionetto, I. Zizzari, M. Salati, A. Pisano, M. Federica, M. Simmaco, M. Nuti and P. Marchetti, *J. Transl. Med.*, 2018, **16**, 1–6.
- D. H. Munn and A. L. Mellor, *Trends Immunol.*, 2013, **34**, 137–143.
- S. Löb, A. Königsrainer, H.-G. Rammensee, G. Opelz and P. Terness, *Nat. Rev. Cancer*, 2009, **9**, 445.
- M. Platten, N. von Knebel Doeberitz, I. Oezen, W. Wick and K. Ochs, *Front. Immunol.*, 2014, **5**, 673.
- Y. W. Moon, J. Hajjar, P. Hwu and A. Naing, *J. Immunother. Cancer*, 2015, **3**, 51.
- J. Godin-Ethier, L.-A. Hanafi, C. A. Piccirillo and R. Lapointe, *Clin. Cancer Res.*, 2011, **17**, 6985–6991.
- C. Uyttenhove, L. Pilotte, I. Théate, V. Stroobant, D. Colau, N. Parmentier, T. Boon and B. J. Van den Eynde, *Nat. Med.*, 2003, **9**, 1269–1274.
- B. C. Creelan, S. Antonia, G. Bepler, T. J. Garrett, G. R. Simon and H. H. Soliman, *Oncoimmunology*, 2013, **2**, e23428.
- H. Liu, Z. Shen, Z. Wang, X. Wang, H. Zhang, J. Qin, X. Qin, J. Xu and Y. Sun, *Sci. Rep.*, 2016, **6**, 21319.
- T. Weng, X. Qiu, J. Wang, Z. Li and J. Bian, *Eur. J. Med. Chem.*, 2018, **143**, 656–669.
- J. E. Cheong and L. Sun, *Trends Pharmacol. Sci.*, 2018, **39**, 307–325.
- A. J. Muller, J. B. DuHadaway, P. S. Donover, E. Sutanto-Ward and G. C. Prendergast, *Nat. Med.*, 2005, **11**, 312.
- M. Li, A. R. Bolduc, M. N. Hoda, D. N. Gamble, S.-B. Dolisca, A. K. Bolduc, K. Hoang, C. Ashley, D. McCall and A. M. Rojiani, *J. Immunother. Cancer*, 2014, **2**, 21.
- M. Liu, X. Wang, L. Wang, X. Ma, Z. Gong, S. Zhang and Y. Li, *J. Hematol. Oncol.*, 2018, **11**, 100.
- G. C. Prendergast, A. Mondal, S. Dey, L. D. Laury-Kleintop and A. J. Muller, *Trends Cancer*, 2018, **4**, 38–58.
- M. L. Bolognesi, *Curr. Med. Chem.*, 2013, **20**, 1639–1645.
- R. R. Ramsay, M. R. Popovic-Nikolic, K. Nikolic, E. Uliassi and M. L. Bolognesi, *Clin. Transl. Med.*, 2018, **7**, 3.
- K. Fang, G. Dong, Y. Li, S. He, Y. Wu, S. Wu, W. Wang and C. Sheng, *ACS Med. Chem. Lett.*, 2018, **9**, 312–317.
- K. Fang, S. Wu, G. Dong, Y. Wu, S. Chen, J. Liu, W. Wang and C. Sheng, *Org. Biomol. Chem.*, 2017, **15**, 9992–9995.
- J. Dong, Q. Zhang, Z. Wang, G. Huang and S. Li, *ChemMedChem*, 2018, **13**, 1490–1507.
- Y. Wan, S. He, W. Li and Z. Tang, *Anti-Cancer Agents Med. Chem.*, 2018, **18**, 1228–1234.
- D.-H. Bach, D. Kim and S. K. Lee, in *Natural Products for Cancer Chemoprevention: Single Compounds and Combinations*, ed. J. M. Pezzuto and O. Vang, Springer International Publishing, Cham, 2020, pp. 469–488.
- N. Pradhan, S. Paul, S. J. Deka, A. Roy, V. Trivedi and D. Manna, *ChemistrySelect*, 2017, **2**, 5511–5517.
- S. Qian, T. He, W. Wang, Y. He, M. Zhang, L. Yang, G. Li and Z. Wang, *Bioorg. Med. Chem.*, 2016, **24**, 6194–6205.



- 34 L. Yang, Y. Chen, J. He, E. M. Njoya, J. Chen, S. Liu, C. Xie, W. Huang, F. Wang and Z. Wang, *Bioorg. Med. Chem.*, 2019, **27**, 1087–1098.
- 35 H. Tsujino, T. Uno, T. Yamashita, M. Katsuda, K. Takada, T. Saiki, S. Maeda, A. Takagi, S. Masuda and Y. Kawano, *Bioorg. Med. Chem. Lett.*, 2019, **29**, 126607.
- 36 A. I. Thaker, M. S. Rao, K. S. Bishnupuri, T. A. Kerr, L. Foster, J. M. Marinshaw, R. D. Newberry, W. F. Stenson and M. A. Ciorba, *Gastroenterology*, 2013, **145**, 416–425.
- 37 M. Ogawa, M. Watanabe, T. Hasegawa, K. Ichihara, K. Yoshida and K. Yanaga, *Mol. Clin. Oncol.*, 2017, **6**, 701–704.
- 38 J. Godin-Ethier, L. A. Hanafi, C. A. Piccirillo and R. Lapointe, *Clin. Cancer Res.*, 2011, **17**, 6985–6991.
- 39 J. E. Cheong, A. Ekkati and L. Sun, *Expert Opin. Ther. Pat.*, 2018, **28**, 317–330.
- 40 D. H. Bach, S. H. Kim, J. Y. Hong, H. J. Park, D. C. Oh and S. K. Lee, *Mar. Drugs*, 2015, **13**, 6962–6976.
- 41 D.-H. Bach, J.-Y. Liu, W. K. Kim, J.-Y. Hong, S. H. Park, D. Kim, S.-N. Qin, T.-T.-T. Luu, H. J. Park, Y.-N. Xu and S. K. Lee, *Bioorg. Med. Chem.*, 2017, **25**, 3396–3405.
- 42 O. Trott and A. J. Olson, *J. Comput. Chem.*, 2010, **31**, 455–461.
- 43 Y.-H. Peng, S.-H. Ueng, C.-T. Tseng, M.-S. Hung, J.-S. Song, J.-S. Wu, F.-Y. Liao, Y.-S. Fan, M.-H. Wu, W.-C. Hsiao, C.-C. Hsueh, S.-Y. Lin, C.-Y. Cheng, C.-H. Tu, L.-C. Lee, M.-F. Cheng, K.-S. Shia, C. Shih and S.-Y. Wu, *J. Med. Chem.*, 2016, **59**, 282–293.

